Cantori barriers in the excitation of a diatomic molecule by chirped pulses

1999 J. Phys. B: At. Mol. Opt. Phys. 32 4001

(http://iopscience.iop.org/0953-4075/32/16/301)

J. Phys. B: At. Mol. Opt. Phys. **32** (1999) 4001–4012. Printed in the UK PII: S0953-4075(99)00704-X

Cantori barriers in the excitation of a diatomic molecule by chirped pulses

J T Lin† and T F Jiang‡§

† Institute of Atomic and Molecular Sciences, Academia Sinica, PO Box 23-166, Taipei 10674, Taiwan

‡ Department of Chemistry, University of Kansas, Lawrence, KS 66045, USA

§ Institute of Physics, National Chiao Tung University, Hsinchu 30050, Taiwan

Received 5 January 1999, in final form 5 July 1999

Abstract. We present a nonlinear dynamical study of a diatomic molecule under the interaction of chirped pulses. The step-like dissociation probability with respect to the initial vibrational states reflects the cantori barriers during the excitation process. The correspondence between classical and quantum cantori barriers is shown through classical phase trajectory and quantum Husimi distribution function. According to the results, the quantum suppression of classical dissociation in molecular excitation by chirped pulse disappears at some field parameters.

1. Introduction

Optimal control of state selective excitation and the dissociation enhancement of diatomic molecules have been the subject of extensive theoretical [1–8] and experimental interest [9–11]. Studies have shown that using a chirped pulse not only significantly reduces the field intensity of the dissociation threshold for a molecule, but also avoids the competitive processes such as ionization and dissociative ionization. In a recent experimental investigation, Maas *et al* [12,13] successfully excited NO molecules from the vibrational ground state to the fifth state in the electronic ground state with a free electron laser. According to their results, the field intensity is moderate and the frequency bandwidth is sufficiently broad to cover several states of the anharmonic vibrational ladder. Therefore, coherent control of molecular excitation by a chirped pulse is feasible.

Theoretically, Liu and Yuan [1, 2] used the bucket dynamics [14] to explain the effective excitation of a chirped pulse by the bucket trapping and convection of classical trajectories. They showed the dissociation probabilities of different initial states, which were divided into soft-chaos and hard-chaos regions with different classical–quantum correspondence. Mishima *et al* [15] used a realistic chirped pulse to study the diabatic coupling of a three-electronic-state one-dimensional (1D) molecular system. They explored the effect of system mass on the laser control of the nonadiabatic process. For lighter mass, it is easier to achieve the population trapping of the electronic excited state by a positively chirped pulse due to its prominent quantum nature.

In the language of nonlinear dynamics [16], the trajectories of an integrable system will be confined in the surface of tori. There is an internal frequency associated with each torus. Under external perturbation, the trajectories begin to move out of the tori and the tori are mostly destroyed as the perturbation increases. However, tori with the most irrational frequency ratio

0953-4075/99/164001+12$30.00

of driving to internal frequency (the so-called winding number) will be persistent and are called KAM tori [17]. The KAM tori will be eventually broken under stronger perturbation [18]. The remnants of these tori form Cantor sets (that is, the cantori) and act as a partial barrier to the stochastic diffusion of phase space trajectories enclosed inside the cantori. The cantori barriers prohibit larger phase volume escape into the chaotic region. Due to the uncertainty principle, the minimum quantum mechanical phase space volume cannot be smaller than the measure of $\bar{h}$. However, there is no limit to how small the phase volume of classical mechanics can be. Consequently, the classical transport probability will be larger than its quantum correspondence and there is *quantum suppression of classical dissociation* in the molecular excitation. Brown *et al* [19] studied this nonlinear dynamical aspect of the suppression phenomenon in the monochromatic light excitation of a diatomic molecule, but no recent study of chirped pulse molecular excitation has been reported to our knowledge.

We recently studied the quantum dynamics of molecular excitation by chirped pulses [20, 21]. We showed that the quantum dissociation probability may be even larger than the classical one for a molecule under the optimal driving field or an adiabatically swept pulse as some field parameters go beyond the thresholds. Because this phenomenon is quite different from the monochromatic light molecular dissociation where quantum suppression of classical dissociation holds, it is worthwhile to examine the dynamics from the point of view of nonlinear dynamics.

Experimental results [22] demonstrated that the linear molecules align along the direction of field polarization and the molecules spend most of their time in this polarization direction. Therefore, for simplicity, investigating the dynamics of diatomic molecules irradiated by the chirped pulse with a 1D model instead of full-dimensional potential is a meaningful work. In fact, the dynamics of full-dimensional and 1D diatomic molecules resemble one another. The major differences are in the magnitude of dipole matrix elements and the selection rules. Although the matrix elements of the full-dimensional potential weaken the dissociation signal with respect to the 1D case, the dissociation dynamics are qualitatively similar [21]. Therefore, it is reasonable to simplify the computation to the 1D model [23, 24].

In the light of the above discussion, this work uses the conventional 1D Morse potential to examine the interaction among diatomic molecules and the external chirped pulse. The relation between the step-like excitation and the classical cantori barriers is described. The results can be compared with study of molecular excitation by monochromatic light (chirp free) in the literature.

In section 2, we briefly describe the approach to the solution of the time-dependent Schrödinger equation and the location of cantori of a 1D Morse potential with external field in phase space. Section 3 then presents quantum and classical results for comparison. Discussions and remarks are included therein. A summary is finally made in section 4.

2. Computation of 1D Morse potential

2.1. Propagation of a wavefunction and its phase space distribution

Under the Born–Oppenheimer approximation, the time-dependent Schrödinger equation for the interaction of a diatomic molecule with an external field under the dipole approximation can be written as:

$$\mathrm{i}\bar{h}\frac{\partial}{\partial t}|\Psi\rangle = \left\{\frac{\hat{P}^2}{2\mu} + \hat{V}(R) - q_e E(t)\cdot R\right\}|\Psi\rangle, \tag{1}$$

where R denotes the centre-of-mass coordinate, and μ represents the reduced mass. $E(t) = E_m U(t) \sin[\Omega_c(t)\, t]$ is the electric field with the chirping frequency $\Omega_c(t)$, where

$$\Omega_c(t) = \Omega_v \left[1 - \alpha_l \left(\frac{t}{T_0} \right)^l \right]. \tag{2}$$

The pulse duration is T_0 and the peak field is E_m. The parameter α_l is defined as the chirping constant of the chirped pulse. In our calculation, we use the linear chirping ($l = 1$) throughout for experimental feasibility. Although calculation [20] indicates that quadratic negative chirping is more efficient to excite the populations than linear chirping, using the linear chirped pulse which is available experimentally [12, 13, 25] is more practical. The case $\alpha_l = 0$ is the chirp-free case. We choose Ω_v to be $1.1\omega_{v,v+1}$, where $\omega_{v,v+1}$ denotes the resonance frequency between the unperturbed vth and $(v + 1)$th states. The optical cycle is defined as $2\pi/\Omega_v$. As is generally known, the vibrational energy level spacings of a Morse oscillator decrease from low to higher states, which explains why the blue-to-red chirping provides a climbing ladder for the pumping process. Additionally, there is an ac-Stark shift for each level, and the π-pulse based upon unperturbed states may not induce an exact population inversion between two neighbouring states [20,21,25]. To compensate for the phase deviation, the initial frequencies adopted herein are $\Omega_c(t = 0) = 1.1\omega_{v,v+1}$ [1, 20].

$U(t)$ is a slowly varying envelope function given by

$$U(t) = \begin{cases} t/t_0 & \text{for} \quad t \leqslant t_0, \\ 1.0 & \text{for} \quad t_0 < t \leqslant T_0 - t_0, \\ (T_0 - t)/t_0 & \text{for} \quad T_0 - t_0 < t \leqslant T_0, \end{cases} \tag{3}$$

where the rising time and switching-off time t_0 is set to ten cycles. The Morse potential is

$$V(R) = D_e\{1 - \exp[-\alpha(R - R_0)]\}^2. \tag{4}$$

We fit the potential parameters to the HF molecular vibrational spectrum such that $D_e = 0.225$, $\alpha = 1.1741$, equilibrium nuclei separation $R_0 = 1.7329$, and reduced mass $\mu = 1744.8423$. Atomic units are used unless otherwise stated. This potential supports 24 bound vibrational levels for the HF molecule. The effective charge q_e is chosen to be $\partial D_p(R)/\partial R|_{R=R_0} = 0.31$ au, where $D_p(R) = 0.4541R \exp[-0.0064R^4]$ denotes a realistic form of dipole moment of HF [8, 19]. Consider a situation in which the intensity is weak or the pulse duration is short, then the linear dipole moment is a good approximation to the first order of the realistic dipole moment [2]. This linear dipole moment is used in classical simulation for simplicity and it is easier to compare its results with quantum calculation in terms of cantori.

The above equation is then propagated by the split-operator spectral method [26] with time increment Δ,

$$\Psi(t + \Delta) = \exp\left[-\mathrm{i}\frac{\hat{P}^2}{4\mu}\Delta \right] \exp\left[-\mathrm{i}\hat{V}_{eff}(R)\Delta \right] \exp\left[-\mathrm{i}\frac{\hat{P}^2}{4\mu}\Delta \right] \Psi(t) + \mathcal{O}(\Delta^3), \tag{5}$$

where the effective potential $V_{eff} = V(R) - q_e E(t) \cdot R$. The state function is transformed alternatively between the coordinate and momentum spaces by fast-Fourier transform that reduces the computational time significantly [27].

With the numerical method described above, the wavefunction can be easily computed at any time, subsequently providing further insight into the dynamics of system evolution. Herein, we calculate the dissociation probabilities of different states versus chirping constant α_l, field strength E_m and its phase space distribution by applying the adaptive grids method used in our previous work [20].

The dissociation probability P_d is defined as,

$$P_d(t) \equiv 1 - \sum_{\nu=1}^{24} P_\nu(t), \tag{6}$$

where $P_\nu(t) = |\langle\phi_\nu|\Psi(t)\rangle|^2$ denotes the population of the νth bound state ϕ_ν of the 1D Morse oscillator at time t.

The quantum analogy of classical phase space distribution for a wavefunction $\Psi(t)$ can be constructed by the Wigner transformation [28],

$$\rho_W(R, P; t) = (1/2\pi\hbar) \int \mathrm{d}R' \, \langle R - \tfrac{1}{2}R'|\Psi\rangle\langle\Psi|R + \tfrac{1}{2}R'\rangle \exp(\mathrm{i}PR'/\hbar). \tag{7}$$

However, since $\rho_W(R, P; t)$ is not everywhere positive, introducing the Gaussian smoothing allows us to obtain a coarse-grained Wigner distribution [29],

$$\rho_H(R, P; t) = (1/2\pi\hbar)|\langle\phi_{\langle r\rangle,\langle p\rangle}|\Psi\rangle|^2, \tag{8}$$

where $\phi_{\langle r\rangle,\langle p\rangle}$ is the minimum wavepacket (coherent state),

$$\phi_{\langle r\rangle,\langle p\rangle}(R) = \frac{1}{[2\pi(\Delta r)^2]^{1/4}} \exp\left\{\frac{\mathrm{i}}{\hbar}\langle p\rangle R - \frac{(R - \langle r\rangle)^2}{4(\Delta r)^2}\right\}, \tag{9}$$

and $\rho_H(R, P; t)$ is the Husimi distribution function [30] that is positive definite.

The following section compares the motion of the Husimi distribution in phase space with the classical phase space distribution under chirped pulses and chirp-free cases.

2.2. Classical simulation and the location of the KAM tori

Mackay *et al* [31] defined the *golden cantori* as the cantori that have irrational winding numbers $n_g + \nu_g$, where n_g denotes a non-negative integer and $\nu_g = (\sqrt{5}-1)/2$. The golden tori inhibit the global stochasticity [23, 32]. For the excitation of a molecule by a chirped pulse, the remaining KAM tori are those golden tori. However, locating such cantori becomes more difficult when the system's degree of freedom is more than two. For simplicity, the cantori in a 1D potential and single mode external field are considered. The classical Hamiltonian for a nonrotating diatomic molecule interacting with a laser field can be written as [33]

$$H_c = H_M + H_F + \lambda H_I = E_{tot}, \tag{10}$$

where H_F and H_M are Hamiltonians for the radiation field and the HF molecule, respectively, and H_I represents the field–molecule interaction.

$$\begin{aligned} H_M &= P^2/2\mu + V(R), \\ H_F &= \tfrac{1}{2}[{P_F}^2 + {\Omega_\nu}^2 {X_F}^2], \\ H_I &= -q_e R X_F, \end{aligned} \tag{11}$$

with coupling parameter λ relating to field strength E_m and intensity I

$$\lambda = \Omega_\nu E_m/\sqrt{2E_{tot}} = \Omega_\nu[I/c\epsilon_0 E_{tot}]^2, \tag{12}$$

where ϵ_0 is the permittivity of free space and E_{tot} ($= 1.427 \times 10^6$ au for $I = 10^{13}$ W cm^{-2}) is the conserved total energy of the laser/oscillator system.

The cantori are then approximated by rational winding number cycles which are continued fractions that converge to $n_g + \nu_g$ [23, 34]. Two cantori exist inside the unperturbed separatrix ($H_M(P, R) = 0$) for HF at $\Omega_{\nu=1}$ and $I = 10^{13}$ W cm^{-2}; one of them has winding number $1 + \nu_g$ and the other is $2 + \nu_g$ [19]. Numerically, the two cantori can be approximated by

F_{k+1}/F_k and F_{k+2}/F_k, respectively, where F_k denotes the kth Fibonacci number. Finding the location of periodic orbits is straightforward by solving the following equation [23]:

$$\begin{aligned} R_n(P_0, R_0) &= R_0, \\ P_n(P_0, R_0) &= P_0, \end{aligned} \tag{13}$$

where R_0 and P_0 refer to the initial estimates for the position and momentum of the periodic orbit on the $X_F = 0$ surface of section, respectively. In addition, R_n and P_n are the position and momentum of the trajectory on its nth pass through the surface of section.

Then, it is instructive to compare the quantum results with the classical ones that reveal the bucket dynamics and dynamical barrier scenarios [19]. The classical dissociation probability is defined from those trajectories that have a total energy greater than zero after turning off the field. In our calculation, a microcanonical ensemble of 1000 points (R, P) is used as the initial values. Each point (R, P) in the ensemble is chosen randomly to satisfy $P^2/(2\mu)+V(R) = E_v$ with $R_1 \leqslant R \leqslant R_2$ where E_v is the eigenenergy of a specified vibrational state, and the classical turning points R_1 and R_2 are the roots of $V(R) = E_v$. The microcanonical ensemble method has been widely used in classical simulation of light–atomic interaction [35] and atomic collisions [36, 37]. In general, a few hundred sampling trajectories are enough to reach convergent results. In our calculation, the use of 1000 initial points or a few hundred less make no difference to our conclusions. These trajectories are calculated from the Hamiltonian–Jacobi equation:

$$\begin{aligned} \frac{\partial R}{\partial t} &= \frac{P}{\mu}, \\ \frac{\partial P}{\partial t} &= \frac{-\partial V(R)}{\partial R} + q_e E(t). \end{aligned} \tag{14}$$

3. Results and discussions

In the following discussions, each state is irradiated by a chirped pulse of intensity 10^{13} W cm^{-2} and duration $T_0 = 120 \times (2\pi/\Omega_v)$, with frequency $\Omega_v = 1.1\omega_{v,v+1}$ where $v = 1, \ldots, 24$ is the vibrational quantum number. The chirping constant is varying, as will be described below. The approximate KAM cantori are located between the eighth and ninth states for $n_g = 1$ and the fourteenth and fifteenth states for $n_g = 2$ with rational numbers $\frac{8}{5}$ and $\frac{13}{5}$, respectively. We first investigate the effect of the two KAM cantori on the dissociation of a diatomic molecule under the irradiation of a chirped pulse. The system is prepared at different vibrational eigenstates. For each initial state under chirped pulse of duration T_0, we check the dissociation probability at the end of pulse. We increase the chirping constant α_l gradually and define the 0.25% threshold chirping constant α_{th} and 5% α_{th} as the dissociation reaches 0.25% or 5%, respectively, at the end of the pulse [38]. Figure 1(a) displays α_{th} at various initial states for both 0.25% and 5% dissociations. The two patterns are similar despite the 20-times difference in magnitude of dissociation probability. For low-lying initial states, larger α_{th} values are required than for higher lying states. Both curves roughly share three different patterns of slope: for initial states lying inside the first KAM tori ($v \sim 8$), for states lying between the first and second KAM tori ($8 < v <$ 12–13), and for the states lying outside both KAM tori (13–14 $< v$). For states in the last category, the dissociation occurs under monochromatic light (chirp free) at intensity 10^{13} W cm^{-2}. Apparently, to dissociate a diatomic molecule at low-lying states with a chirp-free pulse, much stronger intensity is required. However, an ionization process occurs at such a high intensity. Thus, theoretical study of pure dissociation of the diatomic molecule using a high-intensity chirp-free pulse is not physically meaningful, although it has often been used.

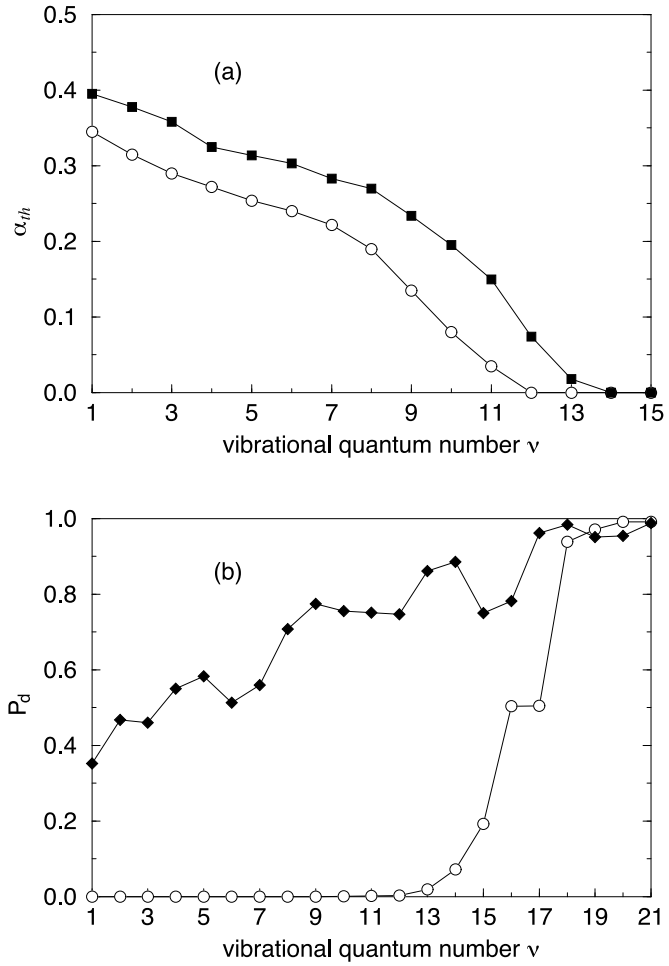

Figure 1. (*a*) Chirping threshold α_{th} versus vibrational quantum number ν for $I = 10^{13}$ W cm^{-2} and pulse duration 120 cycles. Open circles are for dissociation probability equal to 0.25%, full squares are for 5%. (*b*) Dissociation probabilities P_d for different initial vibrational states ν with 120 cycles pulse at intensity 10^{13} W cm^{-2} and chirping constant $\alpha_l = 0.5$. Open circles denote a chirp-free pulse of frequency $1.1\omega_{\nu+1,\nu}$. Full squares are for a chirped pulse with initial frequency $1.1\omega_{\nu+1,\nu}$.

The dissociation probability of the open-circled curve shown in figure 1(*b*) reveals that those states which must pass across more KAM cantori result in a significantly lower dissociation probability than those which just pass one or no KAM cantori when irradiated by a chirp-free pulse. Inside the first cantorus $1 + \nu_g$, the vibrational states have to go through two KAM cantori, and hence it is harder to dissociate. Outside the second KAM cantorus, the dissociation probability rises quickly to saturation as no KAM tori have to be passed through. The plateau regions below $\nu \sim 11$ and $\nu \sim 15$ reflect the fact that the two KAM cantori act the roles of cantori barriers. In contrast, the solid squared curve shows the results when the chirped pulse was used. There is a significant dissociation for each state after the threshold chirping constant is reached. The chirping threshold appears only for states $\nu < 14$ because the states with $\nu > 14$ lie outside the golden KAM cantori and can be dissociated without using

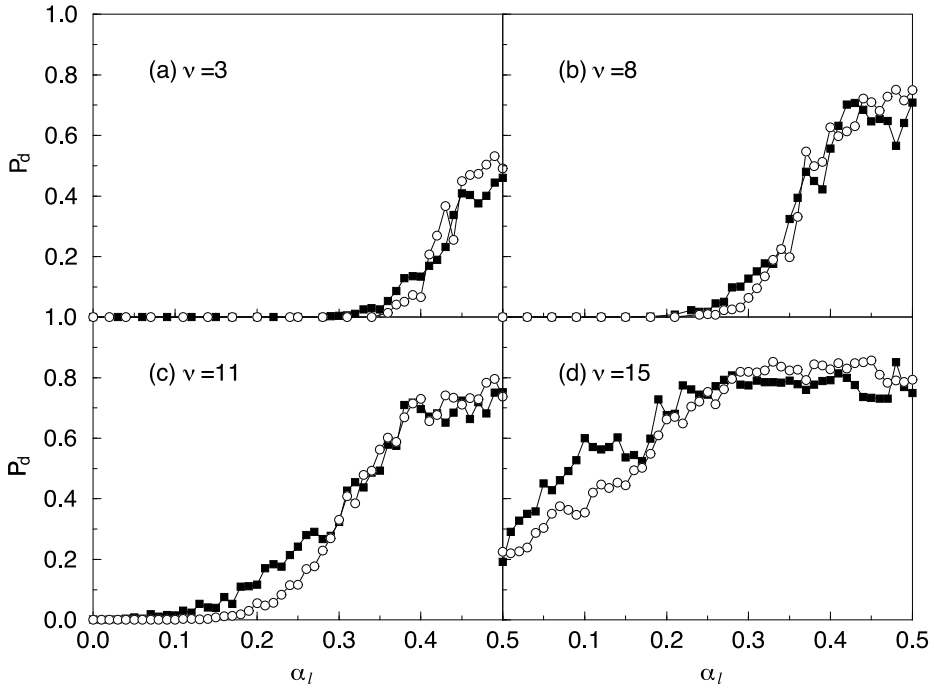

Figure 2. Dissociation probabilities P_d of different vibrational states against chirping constant α_l at $I = 10^{13}$ W cm^{-2} with interaction time 120 cycles of $1.1\omega_{1,2}$. (*a*) The third vibrational state, (*b*) the eighth state, (*c*) the eleventh excited state and (*d*) the fifteenth state. Open circles denote classical simulation and full squares represent quantum calculation.

the chirped pulse, as shown in figure 1(*a*). Therefore, the location of cantori will determine the dissociation dynamics of different initial states which result in the soft-chaos and hard-chaos region and explain the state-dependent classical and quantum results in figure 6 of [2].

In figure 2 we show the variations of dissociation with respect to α_l for several initial states. The results show the following: (i) the dissociation probability rapidly increases and becomes larger as α_l exceeds the threshold except for the fifteenth state where no chirping threshold exists; (ii) as the chirping constant α_l increases, the dissociation probability also increases and finally saturates at a certain value; and (iii) the cantori still act as a partial barrier to the chirped pulse excitation. The saturation is clearer for states with vibrational quantum number $\nu > 8$ than those of $\nu \leqslant 8$ where more than one barrier must be penetrated. For vibrational states higher than $\nu \sim 15$, the populations can be excited quickly and the dissociation saturation is apparent because there is no confinement of the cantori barrier. Also, the coincidence of the dissociation probabilities of both classical and quantum calculation in figure 2 demonstrates the same excitation processes in the classical and quantum interpretations in which the finite value effect of $\overline{h}$ is not the determinate factor of quantum suppression for $I = 10^{13}$ W cm^{-2}. This can be easily seen in figures 2(*a*)–(*d*) for α_l over 0.3.

For illustration, we depict the quantum correspondence of classical phase space distribution. The system starts from the vibrational ground state for quantum calculations, and from an energy specified phase space ensemble for classical simulations. Cases of chirp free and chirping constant $\alpha_l = 0.5$ are both presented. For the chirp-free case, figure 3 shows the classical stroboscopic shots and figure 4 shows its quantum correspondence through

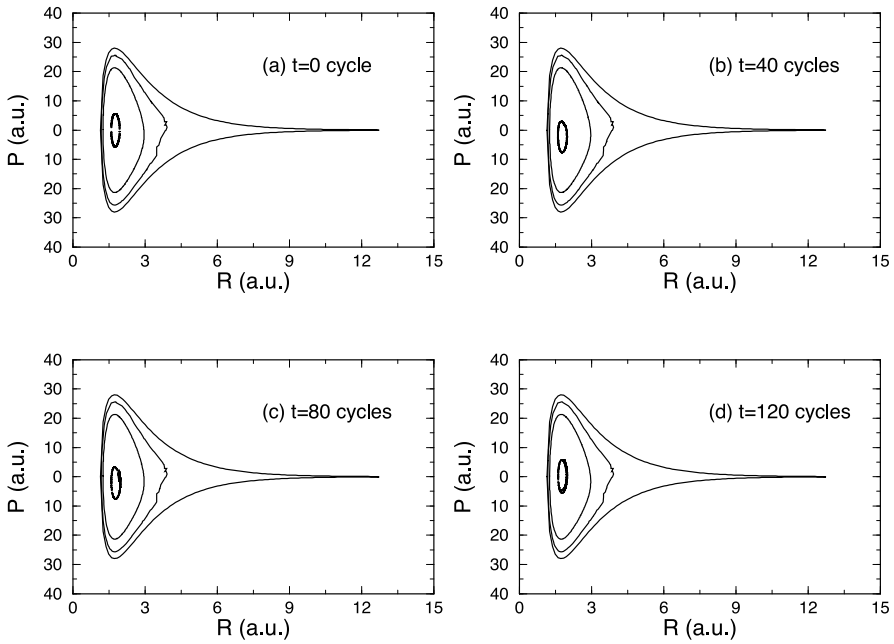

Figure 3. Classical phase space trajectories of the vibrational ground state irradiated by a chirp-free pulse with frequency $1.1\omega_{1,2}$ and pulse duration 120 cycles for $I = 10^{13}$ W cm^{-2} at different times. (*a*) $T_0 = 0$ cycle, (*b*) $T_0 = 40$ cycles, (*c*) $T_0 = 80$ cycles and (*d*) $T_0 = 120$ cycles. Bold solid curves from inner to outer are golden mean cantori and separatrix.

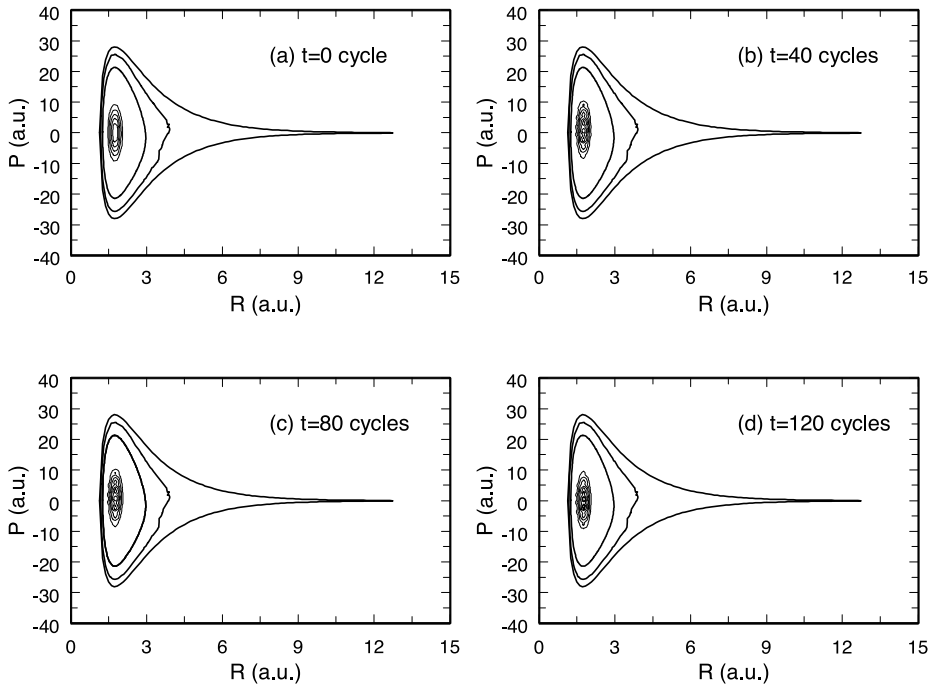

Figure 4. Coarse-grained Wigner distribution of the vibrational ground state irradiated by a chirp-free pulse with frequency $1.1\omega_{1,2}$ and pulse duration 120 cycles for $I = 10^{13}$ W cm^{-2} at different times. The stroboscopic time and the bold solid curves are the same as in figure 3.

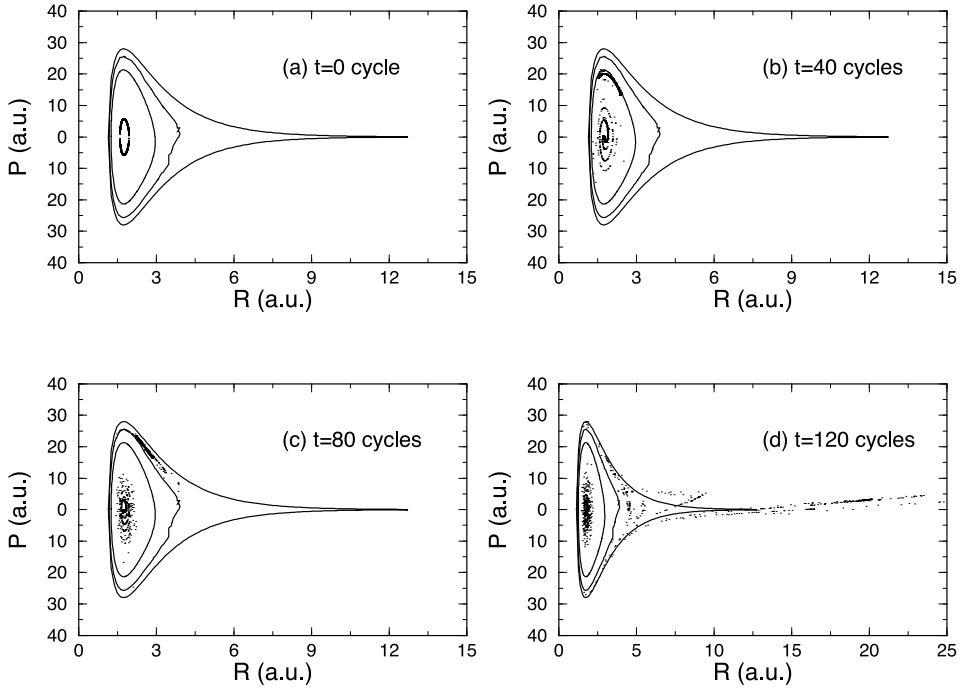

Figure 5. As figure 3, except the chirping constant is $\alpha_l = 0.5$.

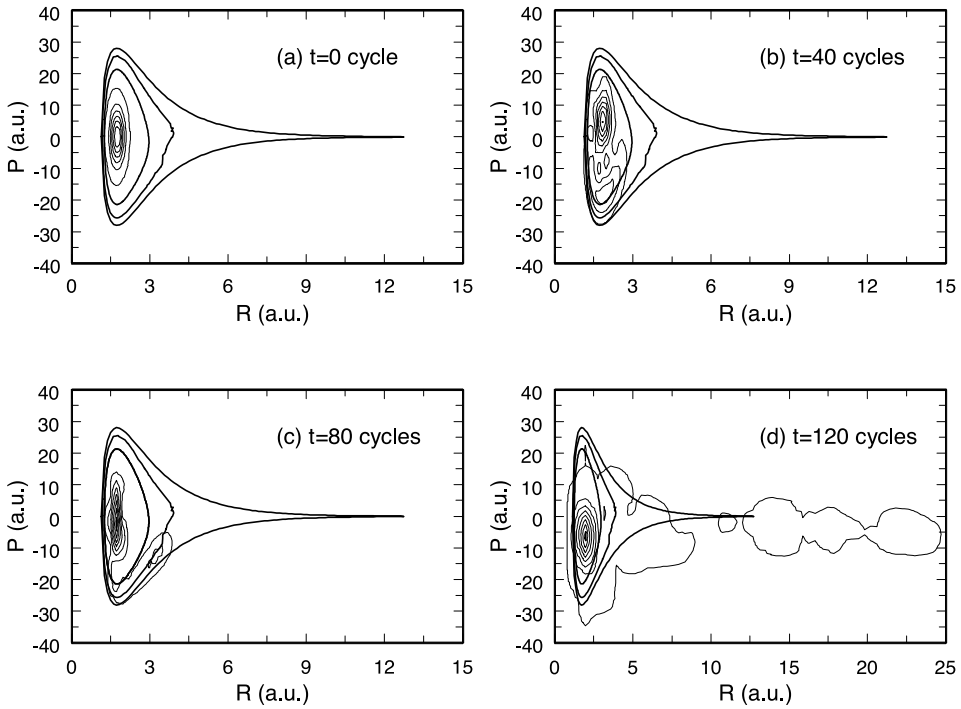

Figure 6. As figure 4, except the chirping constant is $\alpha_l = 0.5$.

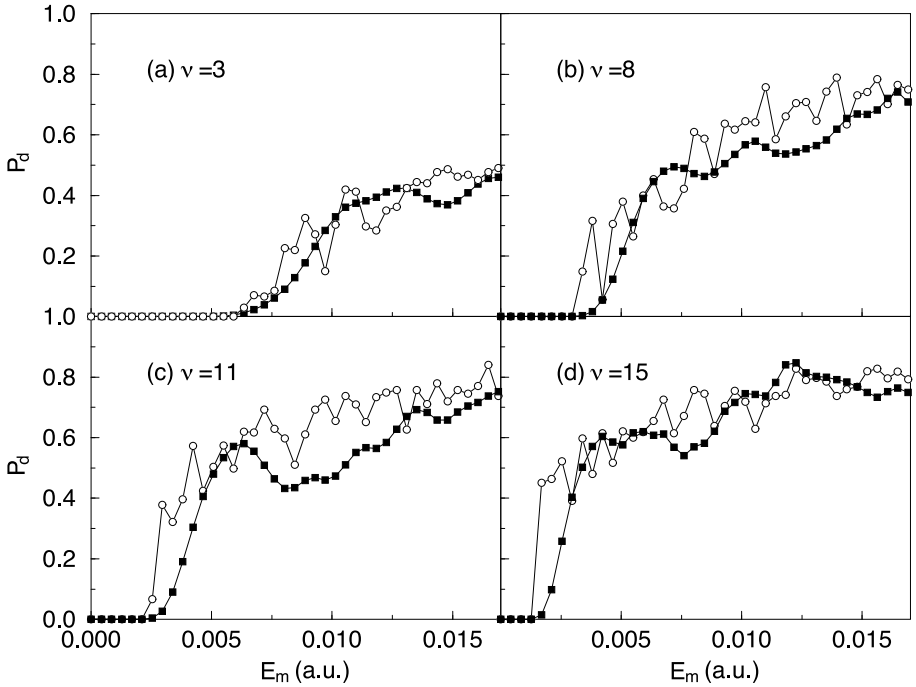

Figure 7. Dissociation probabilities P_d of different vibrational states versus field strength E_m with interaction time 120 cycles and chirping constant $\alpha_l = 0.5$. (*a*) The third vibrational state, (*b*) the eighth state, (*c*) the eleventh state and (*d*) the fifteenth state. Open circles denote classical simulation and full squares represent quantum calculation.

Husimi function. The results reveal that the system remains within the separatrix throughout the pulse duration; thus the dissociation probabilities are zero in both the classical and quantum calculation. Figures 5 and 6 depict the classical and quantum results of chirped pulse cases. The spreading of wavefunction and trajectories in phase space through the golden cantori and separatrix (denoted by darker solid curves) by the chirped pulse is shown. The above findings not only point toward the analogy between chirped pulse excitation of the classical and quantum systems, but also confirm the existence of cantori barriers in quantum dynamics.

Next, we address the question of whether or not the quantum suppression is universal to all field strengths and initial states. To study this problem, we depict the P_d of different vibrational states against field strength E_m for $\alpha_l = 0.5$ in figure 7. The suppression commonly appears at smaller field strengths for all cases on different initial states. But this is not always the case for higher field strengths. When the quantum system is irradiated by a chirped pulse, the suppression disappears as the intensity exceeds the threshold. These results indicate that the *quantum suppression* of classical dissociation is not universal in the excitation of a diatomic molecule by chirped pulses.

Comparing the classical and quantum simulations suggests that chirped pulse excitation resembles the bucket dynamics convection mechanism which provides a path of ladder climbing. The quantum calculation of the dissociation probability is comparable with the classical results only when the chirping rate and/or the intensity exceed the threshold values, whereas monochromatic light excitation acts as the conventional diffusion dynamics of phase space such that the classical dissociation probability is larger than the quantum calculation due to cantori barriers.

4. Conclusions

This study has demonstrated that a linear chirped pulse can more efficiently excite a diatomic system from low-lying states to highly excited states than a chirp-free pulse. By ladder climbing, the systems can be effectively pumped to states outside the golden cantori similar to the classical bucket dynamics. Although the relation between cantori and monochromatic light excitation has been studied by other authors [19], our work discusses the similar dynamics between quantum and classical excitation mechanisms in chirped pulses, which justifies the usefulness of classical calculation when the degree of freedom of the system becomes so large that quantum mechanics cannot cope. Moreover, the quantum suppression of classical dissociation phenomenon due to cantori does not always occur under the chirped pulse excitation. This suppression disappears as the chirping constant or the peak field go beyond some critical values.

Acknowledgment

This work was supported by the National Research Council of Taiwan under contract no NSC88-2112-M009-009.

References

[1] Liu W K, Wu B and Yuan J M 1995 *Phys. Rev. Lett.* **75** 1292
[2] Yuan J M and Liu W K 1998 *Phys. Rev.* A **57** 1992
[3] For a general review, please see, Warren W S, Rabitz H and Dahleh M 1993 *Science* **259** 1581
[4] Chelkowski S, Bandrauk A D and Corkum P B 1990 *Phys. Rev. Lett.* **65** 2355
[5] Chelkowski S and Bandrauk A D 1997 *J. Raman Spectrosc.* **28** 459
[6] Krempl S, Eisenhammer T, Hübler A and Mayer-Kress G 1992 *Phys. Rev. Lett.* **69** 430
[7] Guérin S 1997 *Phys. Rev.* A **56** 1458
[8] Kaluža M, Muckerman T, Gross P and Rabitz H 1994 *J. Chem. Phys.* **100** 4211
[9] Bardeen C J, Wang Q and Shank C V 1995 *Phys. Rev. Lett.* **75** 3410
[10] Melinger J S, Gandhi S R, Hariharan A, Goswami D and Warren W S 1994 *J. Chem. Phys.* **101** 6439
[11] Zhang J, Riehn C W, Dulligan M and Wittig C 1996 *J. Chem. Phys.* **104** 7027
[12] Maas D J, Ducan D I, van der Meer A F G, van der Zande W J and Noordam L D 1997 *Chem. Phys. Lett.* **270** 45
[13] Maas D J, Ducan D I, Vrijen R B, van der Zande W J and Noordam L D 1998 *Chem. Phys. Lett.* **290** 75
[14] Hsu C T, Cheng C Z, Helander P, Sigmar D J and White R 1994 *Phys. Rev. Lett.* **72** 2503
[15] Mishima K and Yamashita K 1998 *J. Chem. Phys.* **109** 1801
[16] Hilborn R C 1994 *Chaos and Nonlinear Dynamics* (New York: Oxford University Press)
[17] Lichtenberg A J and Lieberman M A 1983 *Regular and Stochastic Motion* (New York: Springer)
[18] Chirikov B V 1979 *Phys. Rep.* **52** 263
[19] Brown R C and Wyatt R E 1986 *J. Phys. Chem.* **90** 3590
[20] Lin J T, Lai T L, Chuu D S and Jiang T F 1998 *J. Phys. B: At. Mol. Opt. Phys.* **31** L117
[21] Lin J T, Jiang T F and Chuu D S 1998 *Phys. Rev.* A **58** 2337
[22] Normand D, Lompré L A and Cornaggia C 1992 *J. Phys. B: At. Mol. Opt. Phys.* **25** L497
[23] Davis M J 1985 *J. Chem. Phys.* **83** 1016
[24] Chelkowski S and Bandrauk A D 1993 *J. Chem. Phys.* **99** 4279
[25] Vrijen R B, Duncan D I and Noordam L D 1997 *Phys. Rev.* A **56** 2205
[26] Hermann M R and Fleck J A Jr 1988 *Phys. Rev.* A **38** 6000
[27] Jiang T F and Chu S I 1992 *Phys. Rev.* A **46** 7322
[28] Wigner E P 1932 *Phys. Rev.* **40** 49
[29] Takahashi K and Saitô N 1985 *Phys. Rev. Lett.* **55** 645
[30] Husimi K 1940 *Proc. Phys. Math. Soc. Japan.* **22** 264
[31] Mackay R S, Meiss J D and Percival I C 1984 *Physica* D **13** 55
[32] Bensimon D and Kadanoff L P 1984 *Physica* D **13** 82
[33] Miller W H 1978 *J. Chem. Phys.* **69** 2188

[34] Ott E 1993 *Chaos in Dynamical Systems* (Cambridge: Cambridge University)
[35] Percival I C and Richards D 1975 *Adv. At. Mol. Phys.* **11** 1
Leopold J G and Percival I C 1979 *J. Phys. B: At. Mol. Phys.* **12** 709
[36] Percival I C 1974 *Comput. Phys. Commun.* **6** 347
[37] Cohen J S 1982 *Phys. Rev.* A **26** 3008
[38] Goggin M E and Milonni P W 1988 *Phys. Rev.* A **37** 796